TRANSNAV
http://www.transnav.eu
the International Journal on Marine Navigation and Safety of Sea Transportation
Volume 14 Number 2 June 2020
DOI: 10.12716/1001.14.02.10

Analysis of Tropospheric Contribution to GPS Positioning Error During Tropospheric Cyclone Marcus in 2018

N. Sikirica
Krapina University of Applied Sciences, Krapina, Croatia
M. Horvat
Zagreb University of Applied Sciences, Zagreb, Croatia
D. Špoljar & I. Rumora
University of Rijeka, Rijeka, Croatia

ABSTRACT: GNSS positioning performance assessment is essential for sustainable development of a growing number of GNSS-based technology and socio-economic applications. Case-studies of GNSS positioning performance in critical environments and applications scenarios reveals vulnerabilities of the GNSS Positioning, Navigation, and Timing (PNT) services, and suggest mitigation techniques and GNSS application risk containment. Here we address the case of GPS positioning performance during a devastating tropical cyclone Marcus that hit the greater area of the city of Darwin, Australia in 2018. We identified specific statistical properties of time series of tropospheric contribution to GPS northing, easting, and vertical positioning error that may contribute to understanding of tropospheric effects on GPS positioning performance during a massive weather deterioration in maritime and coastal areas, and analysed their adversarial effects on GNSS-based maritime applications.

1 INTRODUCTION

With satellite navigation as an enabling technology for a growing number of applications, maintaining Global Navigation Satellite Systems' (GNSS) Positioning, Navigation, and Timing (PNT) service has become a necessity. Different GNSS applications require appropriate quality of PNT (GSA, 2018). Studies of GNSS positioning performance in different scenarios of applications thus add to the knowledge base that empowers risk assessment of GNSS utilisation (HM Government Office for Science, 2018).

Tropospheric delay of GNSS signal is caused by its propagation through non-ionised but non-homogenic medium just above the Earth's surface (Hopfield, 1972), (Parkinson, Spilker, Jr., 1996), (Teunissen, Montentbruck, 2017), (Reguzzoni, 2013), (Schueller, 2001). Meteorological parameters, such as air temperature, air pressure, and water vapour partial pressure, determines the delay encountered by satellite signal while propagating through troposphere (Parkinson, Spilker, Jr., 1996), (Teunissen, Montentbruck, 2017), (Schueller, 2001). The GNSS tropospheric delay consists of a dry-air and a wet-air components, with the latter particularly enlarged during weather deterioration (Parkinson, Spilker, Jr., 1996), (Teunissen, Montentbruck, 2017), (Zhou et al, 2017). Tropospheric delay of GNSS signal is then mapped onto GNSS positioning error using the geometry matrix (Filić, and Filjar, 2018).

Here we analysed the dynamics of GPS positioning error due to tropospheric delay for a selected case of tropical cyclone Marcus (Figure 1) that stroke the city of Darwin, Australia in 2018, a devastating tropical cyclone in a coastal region, affecting a range of maritime GNSS applications (BOM, 2018). The aim of research was to study GPS positioning error variations due to tropospheric delay, rather than the GPS tropospheric delay itself. In the approach used, we focused our effort on understanding the GPS positioning error from the perspective of (maritime) navigation and the other GPS applications.

Fast developing and powerful cyclone caused a massive destruction in the area, with rapid changes of meteorological parameters, providing essential case-study to infer GPS positioning performance degradation in a coastal region. GPS positioning error due to tropospheric delay was then mapped on requirements for PNT in maritime sector to estimate risk of GNSS-based application malfunctioning or failure in a maritime sector.

2 METHODOLOGY

Tropospheric contribution to GPS positioning error, which is an amount of GPS positioning error due to tropospheric delay, may be calculated using methodology developed by (Filić and Filjar, 2018) and an additive model, as presented with (1).

$$TROPOerr = Perr_{tropo-uncompensated} - Perr_{tropo-compensated} \quad (1)$$

with:

$TROPO_{err}$ denotes tropospheric contribution to the over-all GPS positioning error

$Perr_{tropo\text{-}uncompensated}$ denotes GPS positioning error without tropospheric corrections applied on GPS pseudoranges before entering the position estimation process (Filić, and Filjar, 2018), (Filić, Grubišić, and Filjar, 2018)

$Perr_{tropo\text{-}compensated}$ denotes GPS positioning error with the Saastamoinen tropospheric corrections applied on GPS pseudoranges before entering the position estimation process (Filić, and Filjar, 2018), (Filić, Grubišić, and Filjar, 2018)

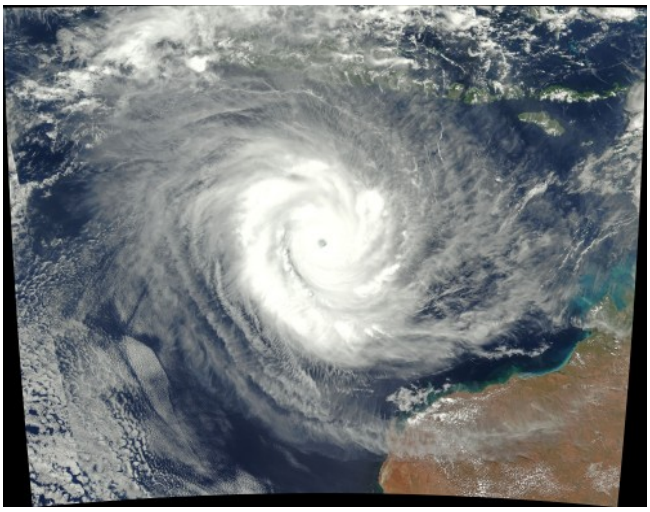

Figure 1. (Source: NASA Earth Observatory, available at: https://eoimages.gsfc.nasa.gov/images/imagerecords/91000/91876/marcus_vir_2018080_lrg.jpg)

The Filić-Filjar methodology (Filić, and Filjar, 2018) (Figure 2) involves: (i) experimental GNSS observations collected by Darwin GNSS reference station (source: International GNSS Service, at: ftp://cddis.gsfc.nasa.gov/gnss/data/daily) during the passage of tropical cyclone Marcus, (ii) post-processing of observations using an open-source GNSS Software-Defined Radio (SDR) receiver RTKLIB (available at: http://www.rtklib.com/) to estimate GPS positioning error as encountered by a commercial grade single-frequency GPS receiver with corrected (compensated)) and uncorrected tropospheric effects (uncompensated), respectively, (iv) statistical analysis of the observed contribution of tropospheric effects of Marcus tropical cyclone to over-all GNSS positioning error, as derived using (1).

Utilisation of GNSS SDR concept allows for a more transparent access to GPS position estimation procedure (Filić, Grubišić, and Filjar, 2018), (Oxley, 2017), (Parknson, Spilker, Jr., 1996), including the control of the pseudorange correction models applied (Figure 3).

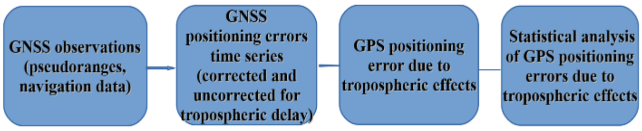

Figure 2. Methodology of research

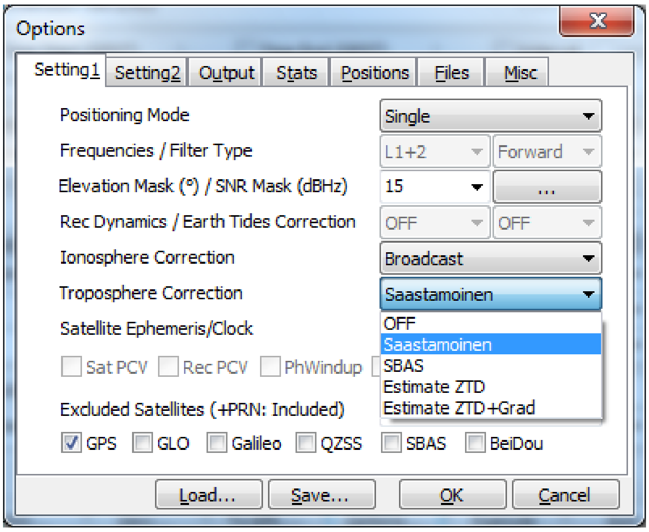

Figure 3. RTKLIB GNSS SDR receiver configuration panel, with available Tropospheric Correction options

Configuration of the GPS SDR RTKLIB framework in post-processing mode ensured it will behave like a common maritime commercial-grade single-frequency GPS receiver. Compensated GPS position estimates were derived by utilisation of Saastamoinen tropospheric correction model (GPS Directorate, 2013), (Filić, and Filjar, 2018), (Parkinson and Spilker, Jr., 1996), (Takasu, 2013), (Teunissen, P J G, Montentbruck, 2017), as given in Eq (2). Saastamoinen model (2) estimates tropospheric delay of the satellite signal, which corrects the raw pseudorange measurements before those serve as the inputs to the GNSS position estimation procedure.

$$T_s^r = \frac{0.002277}{\cos(z)} \cdot \left[p + \left(\frac{1255}{T} 0.05 \right) \cdot e - \tan^2(z) \right] \quad (2)$$

where:

z satellite zenith angle in [rad], defined by elevation angle El^s_r given with (3):

$$z = \frac{\pi}{2} - El_r^s \tag{3}$$

p atmospheric pressure in [hPa], defined by standard Earth atmosphere for the height above the mean geodetic sea level h as with (4):

$$p = 1013.25 \cdot \left(1 - 2.2557 \cdot 10^{-5} \cdot h\right)^{5.2568} \tag{4}$$

T absolute air temperature in [K], defined by standard Earth atmosphere for the height above the mean geodetic sea level h as with (5):

$$T = 15.0 - 6.5 \cdot 10^{-3} \cdot h + 273.15 \tag{5}$$

e … partial water vapour pressure in [hPa], defined by standard Earth atmosphere for the relative humidity h_{rel} given as with (6):

$$e = 6.108 \cdot \exp\left[\frac{17.15 \cdot T - 4684.0}{T - 38.45}\right] \cdot \frac{h_{rel}}{100} \tag{6}$$

Uncompensated tropospheric effects were simulated in RTKLIB environment by utilisation of experimental (observed) GPS pseudoranges with the selection of GPS SDR receiver tropospheric corrections switched off (Figure 3), with the rest of correction models (satellite clocks and ionospheric errors) operational and the receiver configured as a commercial-grade single-frequency ones.

The GPS positioning vector was split into three mutually orthogonal components with roots in the navigation application context: GPS northing, easting, and vertical errors, respectively. Time series of residual GPS positioning errors due to tropospheric effects (1) were analysed using bespoke software developed by (Filić, and Filjar, 2018) in the open-source R environment for statistical computing (available at: https://www.r-project.org/). The analysis comprised (i) the essential statistical analysis, (ii) statistical distribution estimation, through histogram, and (iii) partial auto-correlation analysis (Shumway, and Stoffer, 2017).

3 RESEARCH RESULTS

A rapid weather deterioration increased the level of tropospheric contribution to the over-all GPS positioning error, as depicted in Figure 4.

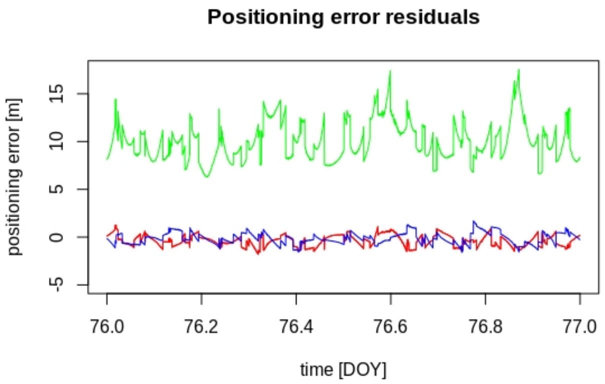

Figure 4. Time series of tropospheric contribution to GPS positioning error components (northing - red, easting - blue, vertical - green, respectively)

Exploratory statistics of time series of GPS positioning error components are presented in Figures 5, 6 and 7, respectively using box-plot diagrams.

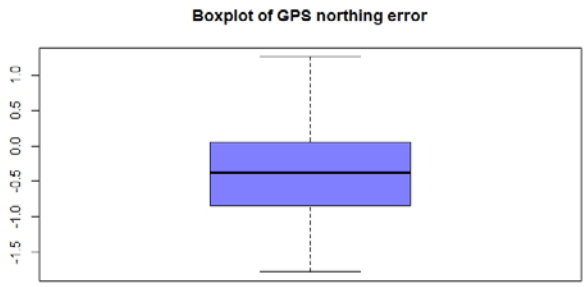

Figure 5. Box-plot summary of GPS northing positioning error component

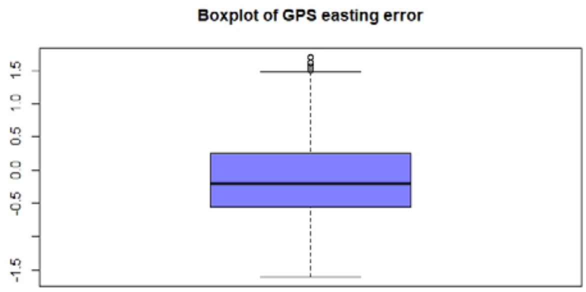

Figure 6. Box-plot summary of GPS easting positioning error component

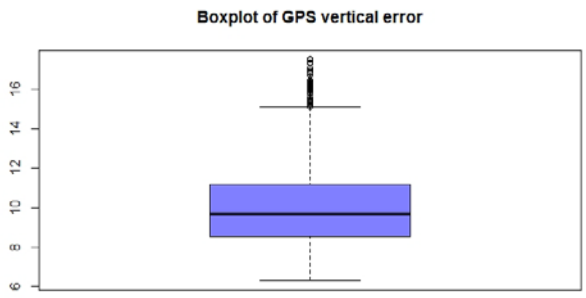

Figure 7. Box-plot summary of GPS vertical positioning error component

Statistical distribution estimation was conducted through histogram analysis, with histograms presented in Figures 8, 9 and 10, respectively.

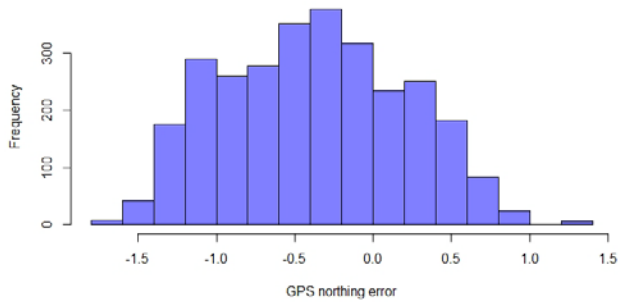

Figure 8. Histogram-based statistical distribution estimates for GPS northing positioning error component

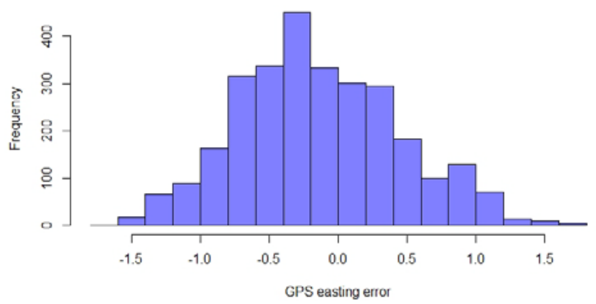

Figure 9. Histogram-based statistical distribution estimates for GPS easting positioning error component

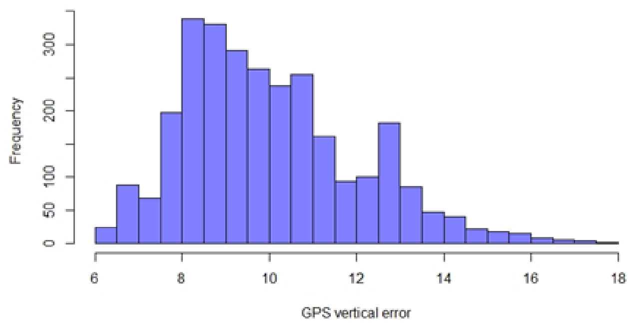

Figure 10. Histogram-based statistical distribution estimates for GPS vertical positioning error component

Figures 11, 12 and 13, respectively, show the Quantile-Quantile (Q-Q) diagrams of time series, for further analysis of statistical distribution of GPS positioning residuals.

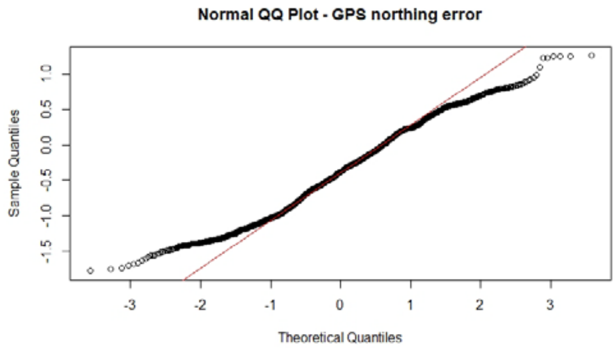

Figure 11. Q-Q diagrams of GPS northing positioning error component

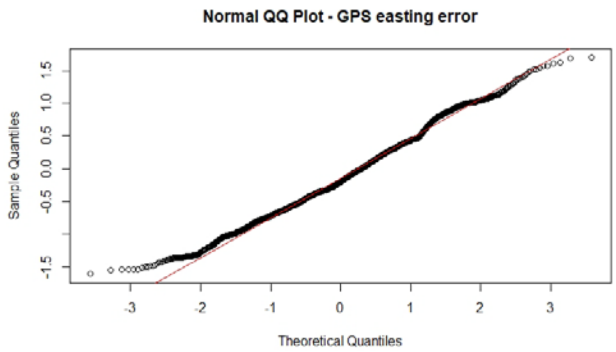

Figure 12. Q-Q diagrams of GPS easting positioning error component

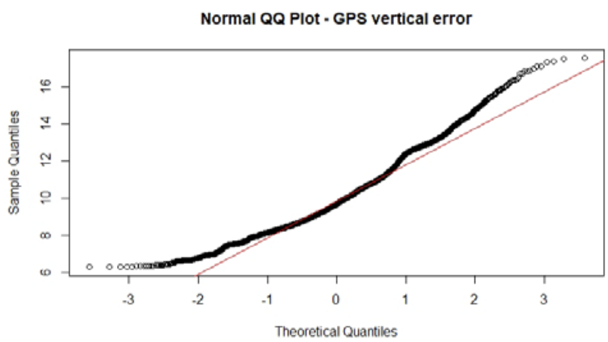

Figure 13. Q-Q diagrams of GPS vertical positioning error component

Finally, Figures 14, 15 and 16, respectively, depicts results of partial auto-correlation analysis of residual GPS positioning error components due to tropospheric effects of tropical cyclone Marcus, derived using partial auto-correlation method.

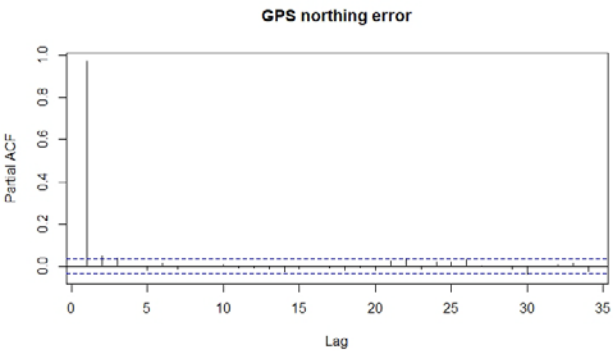

Figure 14. Partial auto-correlation analysis of GPS northing positioning error component

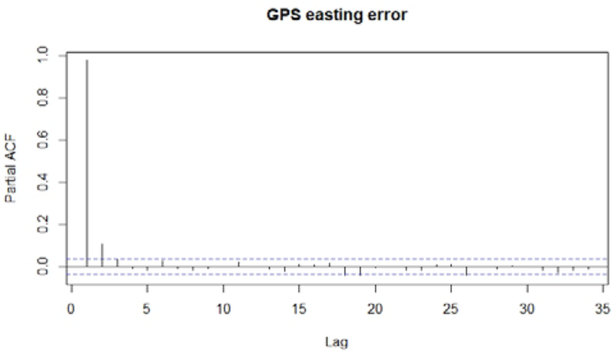

Figure 15 Partial auto-correlation analysis of GPS easting positioning error component

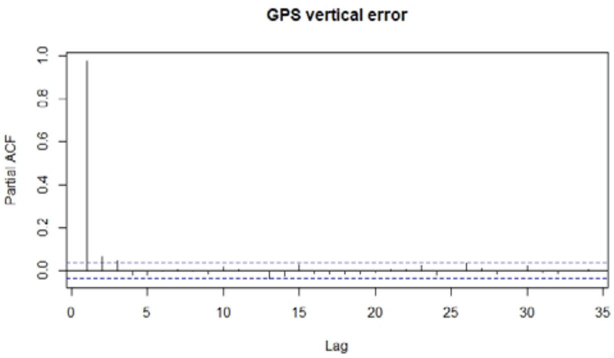

Figure 16. Partial auto-correlation analysis of GPS vertical positioning error component

4 DISCUSSION AND CONCLUSION

The aim of this research was to identify and assess the contribution of the rapidly degrading weather conditions to the GPS positioning error budget of a commercial-grade single-frequency receiver, and address potential implications of neglecting the tropospheric effects for maritime GNSS-based applications.

Based on experimental GPS pseudoranges taken during development of a tropical cyclone, time series of tropospheric contributions to the over-all GPS positioning error vector components (northing, easting, and vertical) were estimated and analysed statistically.

Box-plot diagrams of GPS positioning error components (Figures 5, 6 and 7, respectively) reveal slightly lowered (negative mean) GPS northing and easting positioning error, and enhanced GPS vertical positioning error. GPS easting error box-plot shows an imbalance between mean and median values of the derived time series, with a number of positive outliers.

Histograms and Quantile-Quantile (Q-Q) diagrams (Figures 11, 12, and 13, respectively) (Sumway, and Stoffer, 2017) reveal interesting statistical properties of GPS northing and easting positioning error components. While the histogram of GPS northing positioning error component is suggestive towards normal distribution, the Q-Q plot provides the cues on the contrary. The GPS easting positioning error component time series, although with slightly skewed statistical distribution, yields the Q-Q diagram suggesting good fit with normal distribution. Statistical distribution of GPS vertical positioning error component time series does not follow normal distribution, as it is usually the case in disturbed tropospheric condition (Filić, Filjar, 2018), (Rumora, Jukić, Filić, Filjar, 2018).

Partial auto-correlation-based analysis (Figures 14, 15, and 16, respectively) revealed processes that may be modelled using simple auto-regressive (AR) models, AR(1) for residual GPS positioning northing and vertical errors, and AR(2) for residual GPS positioning easting errors (Shumway, and Stoffer, 2017).

Observed statistical properties will assist in development of appropriate models of GPS positioning performance degradation during rapidly developing and massive weather deterioration, without consideration of the actual GPS tropospheric delay. It should be noticed that we did not analyse the weather deterioration itself, but assessed the consequences on GPS positioning performance only.

Considering required GPS positioning performance in maritime segment (GSA, 2018), we identified a potential issue in utilisation of uncorrected GPS tropospheric delay during a tropical cyclone for port and inland waterways applications. However, the increasing utilisation of unmanned robots (UAVs, autonomous vessels in particular), and the need for relief operation during and in the aftermath of a devastating tropical cyclone in coastal areas may suffer from degraded GPS positioning performance.

We continue our research in examination cases of different weather conditions impact on GNSS positioning performance in maritime areas and for maritime-related navigation and non-navigation applications (Oxley, 2017), (GSA, 2018), in which we will also examine the correlation between the way the weather deterioration develops and the impact on particular components of GPS positioning error vector (Kačmarik et al, 2019).

REFERENCE

BOM. (2018). Severe Tropical Cyclone Marcus. Australian Government, Buraeu of Meteorology (BOM).

Melbourne. VIC. Available at: http://www.bom.gov.au/announcements/sevwx/nt/nttc20180316.shtml

Filić, M and Filjar, R. (2018). A South Pacific Cyclone-Caused GPS Positioning Error and Its Effects on Remote Island Communities. TransNav, 12(4), 663-670. doi: 10.12716/1001.12.04.03

Filić, M, Grubišić, L, and Filjar, R. (2018). Improvement of standard GPS position estimation algorithm through utilization of Weighted Least-Square approach. Proc of 11th Annual Baška GNSS Conference, 7-19. Baška, Krk Island, Croatia. Available at: https://bit.ly/2sLuR82

GSA. (2018). Report on maritime and inland waterways user needs and requirements. European GNSS Agency (GSA). Prague, Czechia. Available at: https://bit.ly/2C7WMVp

Oxley, A. (2017). Uncertainties in GPS positioning: A mathematical discourse. Academic Press/Elsevier. London, UK.

Rumora, I, Jukić, O, Filić, M, and Filjar, R. (2018). A study of GPS positioning error associated with tropospheric delay during Numa Mediterranean cyclone. Int J for Transp and Traff Eng, 8(3), 282-293. doi: 10.7708/ijtte.2018.8(3).03

Schueller,T. (2001). On Ground-Based GPS Tropospheric Delay Estimation (PhD thesis). University of Bundeswehr. Neubiberg, Germany.

Shumway, R H, and Stoffer, D S. (2017). Time Series Analysis and Its Applications with R Examples. Springer Verlag. New York, NY. Available at: http://db.ucsd.edu/static/TimeSeries.pdf